Molecular Therapy
Nucleic Acids
Original Article

Transcriptome Profiling of Neovascularized Corneas Reveals miR-204 as a Multi-target Biotherapy Deliverable by rAAVs

Yi Lu,[1,2,3,4] Phillip W.L. Tai,[4,5,6] Jianzhong Ai,[4,5,6,7] Dominic J. Gessler,[4,5,6] Qin Su,[4,5] Xieyi Yao,[1,2,3] Qiang Zheng,[8] Phillip D. Zamore,[9] Xun Xu,[1,2,3] and Guangping Gao[4,5,6,7]

[1]Department of Ophthalmology, Shanghai General Hospital, Shanghai Jiaotong University, Shanghai 200080, China; [2]Shanghai Key Laboratory of Ocular Fundus Diseases, Shanghai 200080, China; [3]Shanghai Engineering Center for Visual Science and Photomedicine, Shanghai 200080, China; [4]Horae Gene Therapy Center, UMass Medical School, Worcester, MA 01605, USA; [5]Li Weibo Institute for Rare Diseases Research, UMass Medical School, Worcester, MA 01605, USA; [6]Department of Microbiology and Physiological Systems, University of Massachusetts Medical School, Worcester, MA 01605, USA; [7]Department of Urology, Institute for Urology, West China Hospital, Sichuan University, Chengdu, Sichuan 610041, China; [8]Research and Development Center, Chengdu Kanghong Pharmaceuticals Group Co., Chengdu, Sichuan 610036, China; [9]RNA Therapeutics Institute, UMass Medical School, Worcester, MA 01605, USA

Corneal neovascularization (NV) is the major sight-threatening pathology caused by angiogenic stimuli. Current drugs that directly target pro-angiogenic factors to inhibit or reverse the disease require multiple rounds of administration and have limited efficacies. Here, we identify potential anti-angiogenic corneal microRNAs (miRNAs) and demonstrate a framework that employs discovered miRNAs as biotherapies deliverable by recombinant adeno-associated viruses (rAAVs). By querying differentially expressed miRNAs in neovascularized mouse corneas induced by alkali burn, we have revealed 39 miRNAs that are predicted to target more than 5,500 differentially expressed corneal mRNAs. Among these, we selected miR-204 and assessed its efficacy and therapeutic benefit for treating injured corneas. Our results show that delivery of miR-204 by rAAV normalizes multiple novel target genes and biological pathways to attenuate vascularization of injured mouse cornea. Importantly, this gene therapy treatment alternative is efficacious and safe for mitigating corneal NV. Overall, our work demonstrates the discovery of potential therapeutic miRNAs in corneal disorders and their translation into viable treatment alternatives.

INTRODUCTION

Forty million patients worldwide are afflicted by corneal diseases that result in vision impairment or blindness.[1] Corneal neovascularization (NV), the growth of blood vessels into the translucent cornea due to unchecked angiogenesis,[2] is one of the most common pathological changes correlated with the loss of visual acuity.[3] Angiogenesis, in general, is stimulated by several growth factors that are involved in multiple signaling pathways; chief among these is vascular endothelial growth factor (VEGF) signaling.[4] Current anti-VEGF therapeutic strategies to treat corneal NV have been extensively tested in animal models,[5,6] but result in limited efficacies in clinical trials.[7] Small interfering RNAs (siRNAs) against *VEGF* have been demonstrated to reduce corneal NV *in vivo*. However, these effects are only transient and require multiple rounds of administration.[2] These treatment options inherently fall short because they only target one aspect of angiogenesis as a monotherapy. For example, bevacizumab is a therapeutic antibody that only blocks one isoform of VEGF (VEGF-A) and can only prevent the growth of actively growing blood vessels. Even combinatorial delivery of siRNAs to target multiple isoforms of VEGF (1:1:1 mixture of siRNAs targeting VEGF-A, VEGFR-1, and VEGFR-2) still only regulates one pathway that controls angiogenesis.[2] The development of strategies that target multiple pathways driving NV could theoretically circumvent the need for combinatorial therapies.

MicroRNAs (miRNAs) are a class of small non-coding RNAs that function to silence gene expression. miRNAs are involved in nearly every developmental and pathological process, including those involved with angiogenesis.[8,9] Importantly, the control of multiple genes belonging to single or multiple molecular pathways can be regulated by a single miRNA.[10] When delivered and expressed via viral vectors as biotherapies, miRNAs or their precursor forms (pri-miRNAs) may act as "magic bullets" by targeting multiple overlapping or redundant genes that drive a pathological state.

The potential for miRNAs to mitigate angiogenesis in the eye has been explored in many studies. For instance, overexpressing miR-150 was found to have inhibitory effects on mouse retinal NV.[11] More recently, the treatment of corneal NV by an miR-184 mimic was

Received 10 October 2017; accepted 28 December 2017;
https://doi.org/10.1016/j.omtn.2017.12.019.

Correspondence: Guangping Gao, Horae Gene Therapy Center, University of Massachusetts Medical School, 386 Plantation Street, Worcester, MA 01605, USA.
E-mail: guangping.gao@umassmed.edu
Correspondence: Xun Xu, Department of Ophthalmology, Shanghai General Hospital, Shanghai Jiaotong University, No. 100, Haining Road, Shanghai 200080, China.
E-mail: drxuxun@sjtu.edu.cn

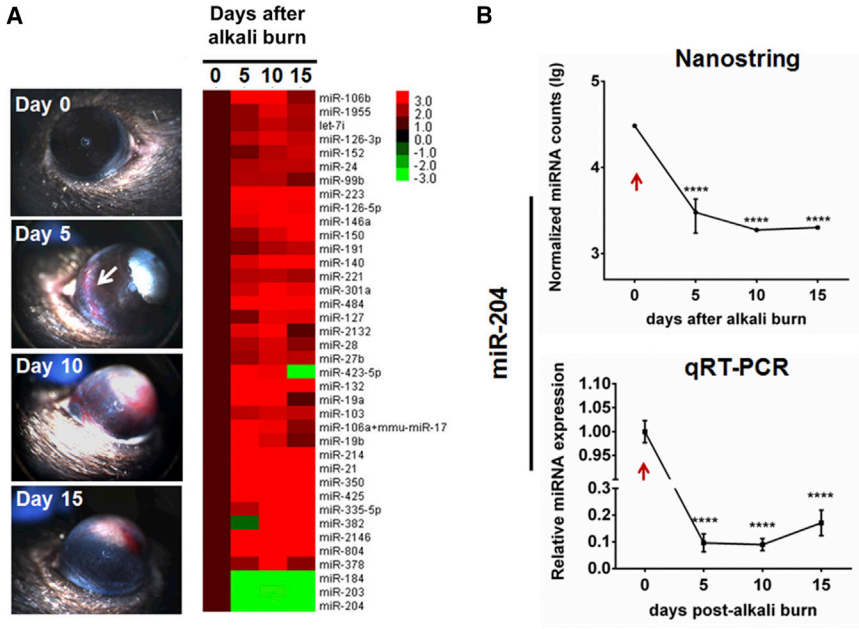

Figure 1. miR-204 Is Significantly Downregulated in Alkali-Burn-Induced Neovascularized Mouse Corneas

(A) miRNA profiling of alkali-burn-induced corneal neovascularization (NV) using NanoString nCounter analysis. Two groups of four pooled corneas were analyzed (eight corneas total). Corneal NV was observed for 15 days after alkali-burn treatment, and corneas from four time points (no treatment [day 0], 5 days, 10 days, and 15 days after treatment) were harvested for RNA extraction. The top 39 differentially expressed miRNAs (see Materials and Methods) are displayed as a heatmap. The color scale is displayed to the right and reflects the fold-change in miRNA expression in alkali-burn-treated corneas compared with untreated corneas. (B) Expression levels (log_{10} scale) of miR-204 following alkali-burn treatment by NanoString nCounter and real-time qPCR analysis. Red arrows at day 0 represent no treatment (harvest before alkali burn). ****$p < 0.0001$ compared with day 0 ($n = 8$/group).

demonstrated in a suture-induced NV model, proving that the delivery of anti-angiogenic miRNAs is a promising means to treat corneal NV.[12] The overall ease of administering viral vectors to the eye makes this type of treatment for corneal diseases an attractive alternative.[13,14] Accordingly, a variety of vectors, techniques, and strategies have been extensively explored.[15] Among these, recombinant adeno-associated viruses (rAAVs) have shown great promise because of their low immunogenicity and genotoxicity profiles, broad tropism, high *in vivo* transduction capacities, and long-term efficacies.[16,17]

We aimed to identify potent therapeutic miRNAs that can be delivered via rAAVs into injured corneas to block angiogenesis. We found that among differentially expressed miRNAs in alkali-burn-induced neovascularized mouse corneas, miR-204 is reduced more than 10-fold in response to alkali-burn injury. Whole-transcriptome analyses and miRNA target prediction identified more than 200 corneal genes that are upregulated in response to alkali-burn treatment and are predicted to be regulated by miR-204. We show that overexpression of pri-miR-204 in injured corneas inhibited vascularization into the cornea via multi-gene targeting. Importantly, we demonstrate that bioinformatic selection of miRNAs expressed in diseased tissues is a promising means of discovering potent genetic regulators of pathological states that can be delivered by safe and efficacious rAAV vectors.

RESULTS

miR-204 Is Significantly Downregulated in Neovascularized Mouse Corneas

We first aimed to identify candidate therapeutic miRNAs that may function to inhibit or reverse corneal NV when overexpressed. We began by characterizing neovascularized mouse corneas induced by alkali-burn treatment. Vascularization into the cornea was observed for 15 days following injury (Figure 1A). Notably, corneal NV was observed to originate in the limbus by day 5 and fully expand into the cornea by days 10 and 15. Untreated corneas and those following 5, 10, and 15 days after alkali-burn treatment were subjected to miRNA profiling using NanoString nCounter analysis. We discovered 36 highly upregulated and 3 strongly downregulated miRNAs in alkali-burn-treated corneas (corneal NV miRNAs) compared with non-treated controls (Figure 1A).

We next aimed to define angiogenesis-related genes that might be directly regulated by corneal NV miRNAs. TargetScan and miRTarBase target prediction yielded a list of 5,520 target genes (Table S1). For this study, we selected miR-204 as the candidate therapeutic miRNAs with the highest potential for inhibiting angiogenesis in the cornea. This reasoning is based on our finding that miR-204 exhibited a >10-fold reduction in neovascularized corneas. Reduction of miR-204 expression was also verified by real-time qPCR (Figure 1B). miR-204 is also conserved across several vertebrate species,[18] making it an ideal candidate for translation into humans. Furthermore, previous studies have shown that miR-204 is downregulated during corneal wound healing[19] and was shown to target Angiopoietin-1 (*angpt1*) during spontaneous corneal NV in the KLEIP-deficient mouse model.[20]

Differential Expression of Predicted miR-204 Target Genes in Alkali-Burn-Treated Corneas Suggests that Multiple Pathways May Promote Corneal NV

We next asked whether miR-204 displays characteristics of a potent therapeutic miRNA for corneal NV. TargetScan and miRTarBase analysis revealed that miR-204 is predicted to target 1,729 genes. Likely, many of these predicted genes may not be expressed in the cornea. Furthermore, only predicted targets that are upregulated in the cornea during alkali-burn treatment would reflect a direct role

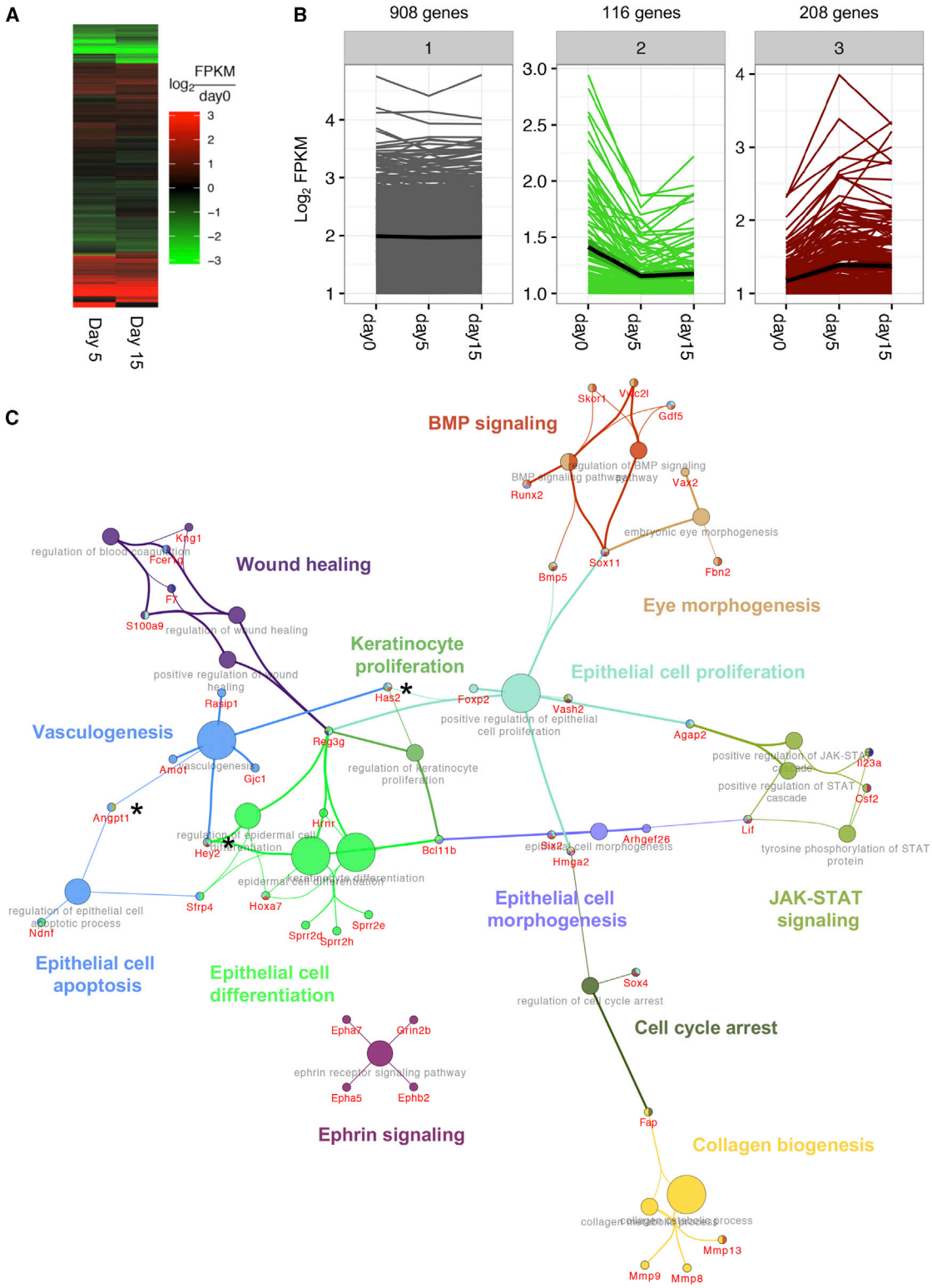

Figure 2. Upregulated miR-204 Predicted Targets Are Associated with Multiple Biological Processes and Pathways

(A) Heatmap of fold-change in expression of miR-204 predicted genes in corneas 5 and 15 days post-alkali-burn treatment. The color scale is displayed to the right. Fold-change is shown as $\log_2$ difference over day 0 values [$\log_2$(fragments per kilobase of transcript per million mapped reads [FPKM]/day 0)]. (B) K-means clustering of miR-204

(legend continued on next page)

for miR-204 in regulating corneal NV. To address this, we performed whole-transcriptome analysis of alkali-burn-treated corneas by RNA sequencing (RNA-seq) analysis. Untreated corneas (day 0) and corneas 5 and 15 days post-treatment (days 5 and 15, respectively) were analyzed. The majority of gene expression changes due to injury, including angiogenesis-related transcripts, occur within the first 5 days of treatment (Figures S1 and S2A). These data suggest that the window for potential intervention is within the first week of injury. We observed that among the 1,729 predicted miR-204 gene targets, 1,232 are differentially expressed in the cornea (Figure 2A). Notably, of the total 448 ontologically annotated angiogenesis-related genes, a subset of the 47 genes is predicted or known to be targets of miR-204 (Figures S2B and S2C). Among these, a few are upregulated upon corneal injury, suggesting that miR-204 may regulate multiple genes in the cornea.

The observation that multiple miR-204 predicted targets were altered during corneal injury prompted us to ask whether miR-204 can impact multiple biological processes in response to alkali burn. Because we were specifically interested in whether downregulation of miR-204 during corneal NV may relieve inhibition of protein-coding genes in response to injury, we focused on the set of genes that were upregulated upon alkali-burn treatment. To this end, we performed k-means clustering and identified 208 genes that were exclusively upregulated in corneas 5 and 15 days post-alkali-burn treatment (Figure 2B). To demonstrate whether these 208 predicted miR-204 target genes might impact multiple genes crucial for mechanisms that are beyond angiogenesis, we subjected these putative targets to gene ontology (GO) term enrichment analysis. By selecting on KEGG pathway and ontological terms closely related to proliferation, for example, wound healing, apoptosis, cell morphogenesis, as well as vasculogenesis, we identified several upregulated miR-204 predicted targets that demonstrate miR-204 as a potent anti-angiogenic effector (Figure 2C; Table S2). Specifically, the vasculogenesis-related genes were identified: Hey2, Gjc1, Angpt1, Has2, Rasip1, and Amot (Figure S3). Interestingly, Angpt1, Has2, and Hey2 also enrich for epithelial cell- or keratinocyte-related ontology terms (Figure 2C), suggesting that miR-204 directly regulates key genes with diverse roles in angiogenesis and cell proliferation in the cornea.

Both Intrastromal and Subconjunctival Delivery of rAAVrh.10 Efficiently Transduces Normal and Alkali-Burn-Treated Corneas

We next aimed to deliver miR-204 into corneal tissues as a biotherapy. At present, rAAVs are the most efficacious and safe vehicles for providing long-term therapeutic transgene expression in the cornea.[21] Thus, we aimed to establish the parameters for potent rAAV transduction in the corneas of normal and alkali-burn-treated eyes. Our previous findings indicated that among a large panel of rAAV serotypes, rAAVrh.10 exhibited the highest transduction efficiency in the corneal stroma by intrastromal injection.[22] Based on these results, we first compared the efficacy of rAAVrh.10 delivery by two different routes of administration: intrastromal and subconjunctival. Both methods are proven routes for rAAV transduction to the cornea, where keratocytes are targeted by rAAV8 with high efficiency.[21] However, because NV originates from the limbus, administration to the subconjunctiva of the eye immediately following injury may be preferred. Notably, subconjunctival injections of bevacizumab results in better prognoses for corneal transplantation by preventing corneal NV-related graft failure.[23] Assessment of rAAVrh.10 transduction efficiency in normal mouse corneas by either intrastromal or subconjunctival injections suggests that both injection methods to deliver rAAVrh.10 EGFP vectors can efficiently transduce the entire cornea (Figures 3A and 3B).

We next evaluated the effects of alkali burn on the efficacy of corneal transduction by rAAVrh.10 vectors (schematized in Figure 3C). Because transgene expression reaches peak levels 2 weeks after intrastromal injection,[22] treatments were performed 2 weeks prior to alkali-burn induction. Subconjunctival injections were performed directly following alkali burn. Whole flat-mount immunofluorescence analyses of eyes harvested 1 or 2 weeks after alkali burn show that EGFP transgene expression in non-alkali-burn-treated corneas (control group) is strongly detected at weeks 1 and 2 with little change in expression for both intrastromal and subconjunctival vector injections (Figure 3D). However, alkali-burn-treated corneas showed robust EGFP expression at week 1 following alkali-burn treatment, but exhibited an extreme loss of EGFP expression at week 2 (Figure 3D).

Quantitative analysis of vector genomes delivered by either intrastromal or subconjunctival injection indicated that rAAV genome copies in alkali-burn-treated corneas were significantly lower than uninjured corneas (Figure 3E). Strikingly, quantification of EGFP mRNA expression showed that there was no significant difference between alkali-burn and control groups at post-alkali-burn week 1; however, EGFP expression in alkali-burn-treated corneas after 2 weeks were significantly lower than control corneas (Figure 3F). Our findings demonstrate that alkali burn severely compromises the expression of rAAVrh.10-delivered transgenes by 2 weeks. Nevertheless, what remains promising for this delivery approach is that differences in transgene expression between normal corneas and treated corneas are negligible for at least 1 week after alkali burn following only a single treatment. This time frame is within the therapeutic window as suggested by our transcriptome data (Figure S1).

rAAVrh.10-Mediated miR-204 and miR-184 Overexpression by Subconjunctival Injection Inhibits Corneal NV

The administration scheme by subconjunctival delivery following corneal injury is more therapeutically relevant. Thus, pri-miR-204

predicted target gene expression profiles in alkali-burn-treated corneas. Three distinct groups were defined: genes with little or no change (left plot, group 1), downregulated genes (center plot, group 2), and upregulated genes (right plot, group 3). (C) Gene ontology (GO) network map for the group 3 genes. Genes that enrich for selected terms are displayed as small nodes that connect to the larger GO-term nodes. The relative sizes of the GO-term nodes also reflect their significance levels. Genes of particular interest that are related to vasculogenesis (Angpt1, Hey2, and Has2; asterisks) are also related to epithelial cell or keratinocyte terms.

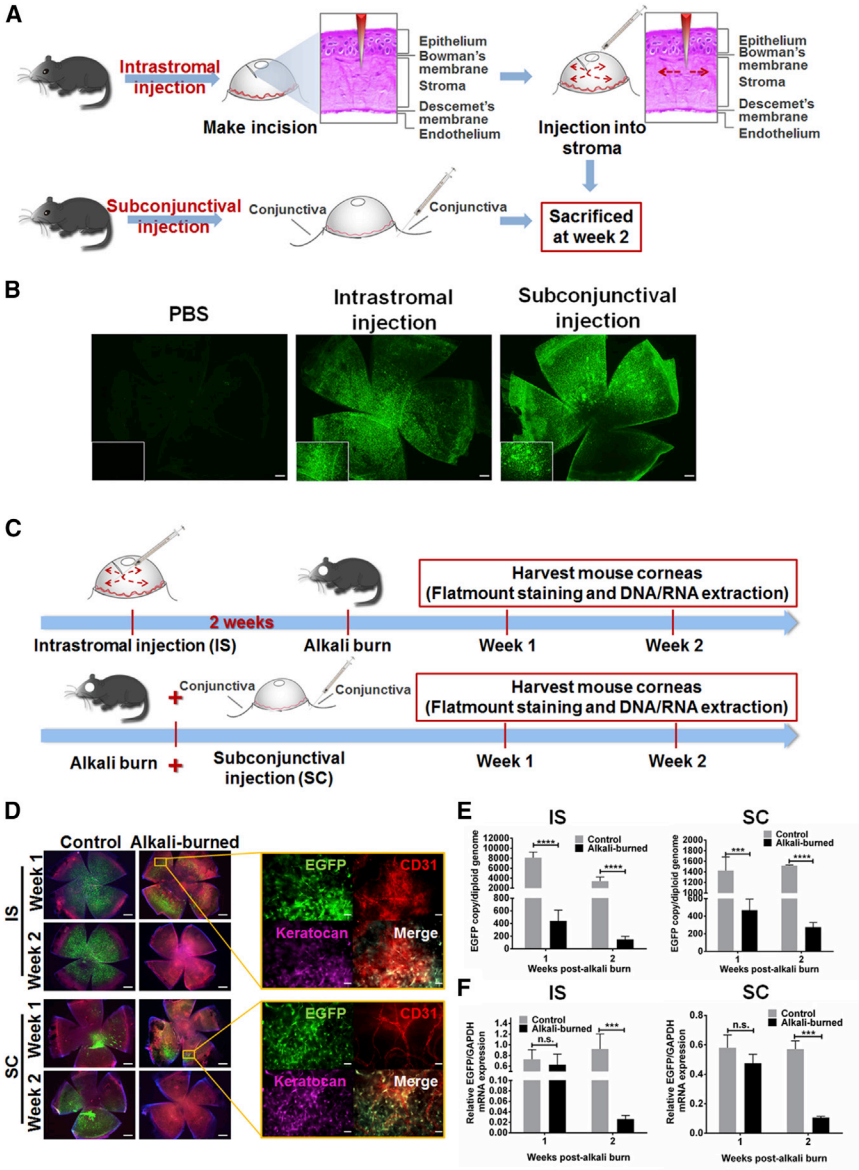

Figure 3. Both Intrastromally and Subconjunctivally Delivered rAAVrh.10 Vectors Efficiently Transduce Normal and Alkali-Burn-Treated Corneas

(A) Diagram of the experimental design to inject rAAVrh.10 EGFP into normal mouse cornea by intrastromal or subconjunctival delivery. (B) Both intrastromal and subconjunctival injections of rAAVrh.10 EGFP show high EGFP expression in mouse corneas. Original magnification ×25; scale bars, 250 μm. Insets: images of the central cornea at ×100 original magnification. (C) The experimental design of intrastromal or subconjunctival injection of rAAVrh.10 EGFP into mouse cornea with alkali burn. (D) Immunofluorescence analysis of mouse corneal flat-mounts. The corneas of control and alkali-burn groups were harvested at weeks 1 and 2 after alkali burn. Green: EGFP; red: CD31 (cell marker of vascular endothelial cells); magenta: keratocan (cell marker of keratocytes). Panels of merged immunofluorescent (IF) images highlight EGFP expression overlapping keratocan-stained cells and not $CD31^+$ cells, showing that EGFP was mainly expressed in keratocytes and not in vascular endothelial cells. Left panels: original magnification ×25; scale bars, 500 μm. Right panels: original magnification ×200; scale bars, 50 μm. (E) Droplet digital PCR (ddPCR) assessment of rAAV genome copy number. (F) The EGFP mRNA expression analysis between alkali-burn-treated and control groups at weeks 1 and 2. n = 8/group. IS, intrastromal injection; n.s., no significant difference; SC, subconjunctival injection. ***$p < 0.001$; ****$p < 0.0001$.

was constructed into rAAVrh.10 vectors and injected into the subconjunctiva of mouse eyes (Figure 4A). *In vivo* tracking of corneal NV progression indicated an inhibition of NV areas after 7 days of mock (vector backbone) and pri-miR-204 treatments (Figure 4B). The NV area in the mock treatment group recovered to those of PBS treatments by day 10, while pri-miR-204 treatments resulted in significantly less NV. Differences in corneal NV after 15 days of treatment with pri-miR-204 as assessed by immunofluorescence analyses in flat-mounts were more definitive (Figures 4C and 4D). Corneas immune-stained with anti-CD31 demonstrated that new blood vessels grew robustly in PBS and mock control groups, while corneas treated with pri-miR-204 vectors effectively inhibited corneal NV. Gross *in vivo* observation and histopathological analysis of corneas and retinas showed no obvious abnormalities or inflammatory response 1 and 2 weeks following injection when compared with control groups (Figure 5).

Delivery of the Anti-angiogenic miR-204 Transgene Targets the Angpt1/Tie2/PI3K/Akt Pathway in the Cornea

We next aimed to demonstrate that blockage of corneal NV by rAAV delivery of pri-miR-204 directly impinges on NV by inhibiting gene pathways known to drive angiogenesis. Alkali-burn-treated mice were injected with rAAVrh.10 pri-miR-204 vectors subconjunctivally as described above. Analysis of miR-204 expression in NV corneas showed that levels were significantly upregulated in the pri-miR-204 treatment group compared with the PBS treatment group in both intrastromal and subconjunctival delivery routes (Figure 6A). The levels of exogenous miR-204 after vector injection and alkali burn alone were still below those of normal control levels. As stated before, Angpt1 has established roles in angiogenesis and wound healing in the cornea via activation of the phosphatidylinositol 3-kinase (PI3K)/AKT signaling pathway.[20,24] Our results indicate that *angpt1* and *vegf* (downstream target gene of PI3K/Akt pathway) messages were significantly downregulated with rAAVrh.10-pri-miR-204 treatments compared with the PBS group (Figure 6B). Western blot analysis confirms that ANGPT-1 and VEGF are significantly reduced by exogenous expression of miR-204, while TIE2 (receptor for

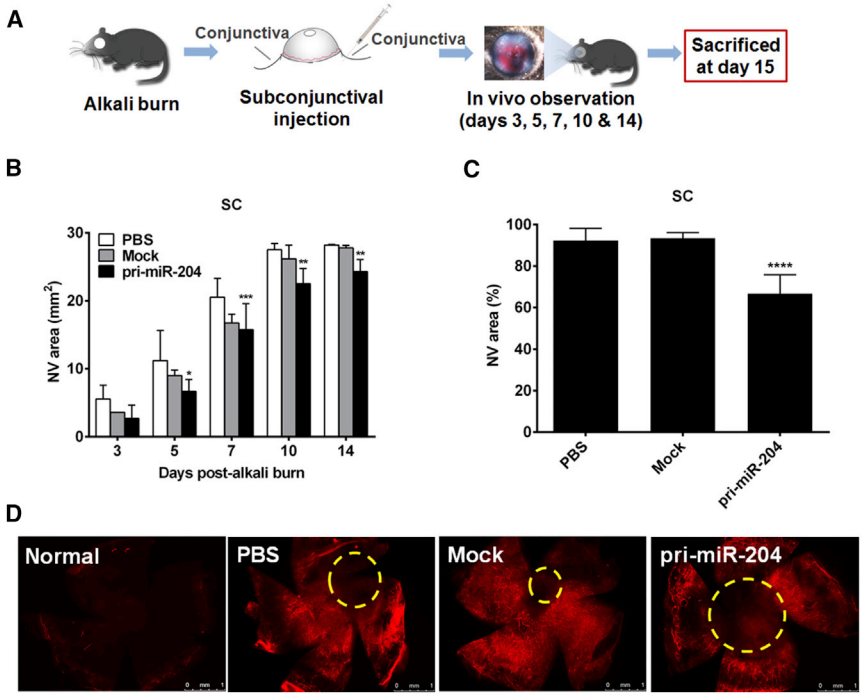

Figure 4. Subconjunctival Injection of rAAVrh.10 Vectors Expressing Pri-miR-204 Inhibits Corneal NV

(A) Diagram of the experimental design. (B) Corneal NV was observed and measured at days 3, 5, 7, 10, and 14 following alkali-burn treatments. (C) Quantification analysis of NV area percentages among CD31-stained whole corneal flat-mounts comparing PBS, mock, and pri-miR-204 treatment groups. Mock: vector backbone without the pri-miR-204. (D) CD31-stained whole corneal flat-mounts harvested 15 days following alkali burn. Blood vessels (CD31-positive) in corneal stroma are stained red. Yellow dashed circles roughly mark the edges of avascularized areas. Original magnification ×25. Scale bar, 1 mm. n = 10/group. *p < 0.05; **p < 0.01; ***p < 0.001; ****p < 0.0001, compared with PBS group.

ANGPT1), PI3K, and AKT demonstrated a loss of phosphorylation without significant reduction in protein expression (Figure 6C).

Delivery of Pri-miR-204 Represses Multiple Genes that Are Upregulated during Corneal NV

To demonstrate the ability for miR-204 to act upon multiple pathways that impact corneal NV, we performed qPCR analysis to assess whether treatment with rAAV-pri-miR-204 can normalize gene targets that were differentially expressed upon corneal injury. As mentioned above, RNA-seq analysis and miR target prediction identified *hey2*, *gjc1*, *has2*, *rasip1*, and *amot* as significantly upregulated during the NV of corneas (Figures 2C and S3). Aside from *hey2*, qPCR analyses of these transcripts in corneas injured by alkali burn (PBS and mock conditions) consistently showed increases in expression at 5, 10, and 15 days post-treatment (Figure 7). Animals that were treated with rAAV-pri-miR-204, on the other hand, showed normalization of transcript levels that returned expression levels to those observed in untreated corneas (Figure 7).

DISCUSSION

Current therapeutic strategies that directly target VEGF to inhibit angiogenesis in corneal NV have yet to show efficacious reversal of the pathology. This challenge is mainly due to the fact that multiple molecular pathways are known to induce angiogenesis. Because current drugs can only target single genes, combinatory therapies may be required for these approaches. Furthermore, pre-existing strategies require repeated administration for complete beneficial outcome, burden the patient, and may become costly with repeated treatments.

In this study, we have aimed to reveal candidate therapeutic miRNAs with strong anti-angiogenic properties. To this end, we have profiled for the first time the global expression of miRNAs in neovascularized mouse corneas induced by alkali-burn treatment, and have performed RNA-seq to identify differentially expressed genes in these tissues. By profiling only those differentially expressed genes that are predicted targets of corneal NV miRs, we now provide a resource for the further discovery of therapeutic miRs that can directly regulate gene expression in the injured mammalian cornea.

Additionally, we show that miR-204 is effective in targeting newly discovered transcripts that are upregulated in vascularized corneas. Of particular note, *Has2* showed a several-fold increase after alkali-burn treatment. This gene is known to be involved in vasculogenesis, keratinocyte proliferation, and epithelial cell proliferation, as indicated by ontological enrichment analysis. Incidentally, it was reported that overexpression of miR-204 could also inhibit corneal epithelial cell proliferation by an unreported mechanism.[19] The capacity for rAAV-pri-miR-204 to return *has2* levels and others back to those of normal corneas suggests that miR-204 can act not only on multiple genes during NV, but also intervene in multiple biological pathways. This ability demonstrates miRNAs as potent and favorable gene therapy alternatives for corneal NV that specifically overcomes the need for multiple treatment strategies required for anti-VEGF therapies. At the time of our findings, a study had demonstrated the effect of miR-184 mimics on corneal NV.[12] We also identified miR-184 to be strongly downregulated upon corneal alkali burn (Figures 1A and S4A). When delivered by rAAVrh.10, miR-184 also has the capacity to attenuate corneal NV. These experiments were carried out in parallel to rAAV-pri-miR-204 experiments and are presented as Figures S4 and S5.

We were able to achieve substantial miRNA expression in injured corneas for 1 week after only a single treatment. Although levels were still lower than those observed in non-damaged corneas (Figures 6A and

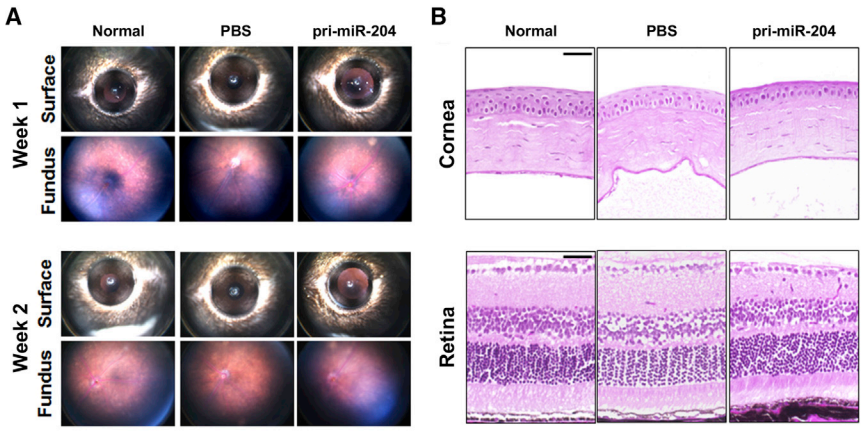

Figure 5. Subconjunctival Injection of rAAVrh.10 Pri-miR-204 Vectors Is Safe for Ocular Tissues

(A) *In vivo* observation of mouse eyes 1 and 2 weeks following PBS or vector injection. (B) Histopathological analysis of corneas and retinas at 2 weeks following PBS or vector injections showed no obvious abnormalities.

S5A), significant anti-angiogenic effects were observed. Despite these less than perfect findings, the results are still clinically meaningful, because transgene products delivered by rAAVs have prolonged outcomes.[21] This feature circumvents the need for repeated drug administrations required by alternative strategies. Furthermore, we show that transgene expression in the cornea is not indefinite. It is plausible that the keratocytes, which are exclusively transduced by rAAVrh.10 in the cornea (Figure 3D), are turned over upon alkali-burn treatment, causing eventual loss of episomal rAAV genomes. This finding highlights a distinct advantage for rAAV-mediated gene therapy; the episomal nature of rAAVs makes them ideal for transiently treating acute corneal diseases.[22] Whether overexpression of exogenous miR-204 by rAAV delivery may negatively impact other cellular processes in non-corneal tissues has yet to be explored. Indeed, the angiogenesis-related gene Hif-1α is known to stimulate miR-204 expression, which in turn leads to the downregulation of the apoptotic protein BCL-2 in neuronal cells.[25] Any cytotoxic outcomes due to rAAV-miR-204 treatment in the surrounding site of injection warrant future exploration. We have shown evidence that at least in the fundus/retina and the cornea, there were no clear tissue abnormalities following injection of rAAV (Figure 5). These data show that the treatment regimen described in our study did not result in noticeable cellular toxicity.

Despite the striking decrease in Akt and β-catenin pathways following pri-miR-204 treatment, as well as normalization of genes involved in vasculogenesis and cell proliferation in the cornea, we did not observe a full reversal or prevention of NV. This partial inhibitory effect might indicate that miR-204 overexpression alone is not sufficient to entirely block NV in the cornea. By comparison, our demonstration of pri-miRs to reverse NV or block NV onset as a prophylactic (Figure S6) underperforms compared with anti-VEGF strategies as demonstrated by Papathanassiou et al.,[6] where subconjunctival injections into rabbits 1 day after alkali burn results in 4.7% NV of the cornea. In that study, however, vascular regression was confined to minor vessels, and blockage of NV occurred only with new vessels. In addition, 2 weeks following treatment, NV into the cornea still developed to a degree, suggesting that multiple administration of drug is required. Importantly, in the same study, scarring of the cornea was not reversed. During the course of our own investigation, we anecdotally observed that some mouse corneas exhibited less fibrotic tissue after treatment of pri-miR-204, but these numbers were not robust enough to conclusively demonstrate reduction of fibrosis. Whether miR-204 or other corneal miRNAs are capable of attenuating corneal scarring merits further investigation. Notably, multiple genes related to wound healing and apoptosis were observed to be upregulated (Table S2). Future studies to validate these as causative targets in rAAV-miR-204 treatments would provide proof for miR-204's utility as the ideal therapeutic miR for treating corneal NV. Candidate genes such as Has2, which we showed was upregulated upon corneal injury, is related to keratinocyte and epithelial cell proliferation, and can be normalized by rAAV-miR-204 (Figure 7), might be key therapeutic targets for reversing fibrosis. Nevertheless, by profiling differentially expressed miRNAs and protein coding transcripts in corneal tissue following alkali-burn-induced NV, we have opened the possibility for the discovery of additional therapeutic transgene strategies via single or even mixed-vector strategies to further boost therapeutic potential for mitigating the development of corneal NV.

MATERIALS AND METHODS

Animals

Six- to eight-week-old female C57BL/6J mice (Charles River Laboratories) were maintained and used according to the guidelines of the Institutional Animal Care and Use Committee (IACUC) of the University of Massachusetts Medical School. All animal experiments conformed to the Association for Research in Vision and Ophthalmology (ARVO) Statement for the Use of Animals in Ophthalmic and Vision Research. Prior to experimental procedures, all animals were anesthetized by intraperitoneal injection of a ketamine-xylazine mixture (100 and 10 mg/kg, respectively).

Mouse Corneal NV Induced by Alkali Burn

Alkali-burn treatments were conducted following previously published methods.[26] Only the right eyes of mice were treated to conform to animal welfare standards required by IACUC and ARVO. Filter-paper discs (3-mm diameter) were pre-soaked in 1 M NaOH for 15 s and applied to eyes in experimental groups for 20 s. The ocular surface was then washed with 15 mL of normal saline for 1 min. A single investigator performed all of the described procedures to ensure reproducibility. Mouse corneas of anesthetized animals were imaged and acquired with a Micron III camera

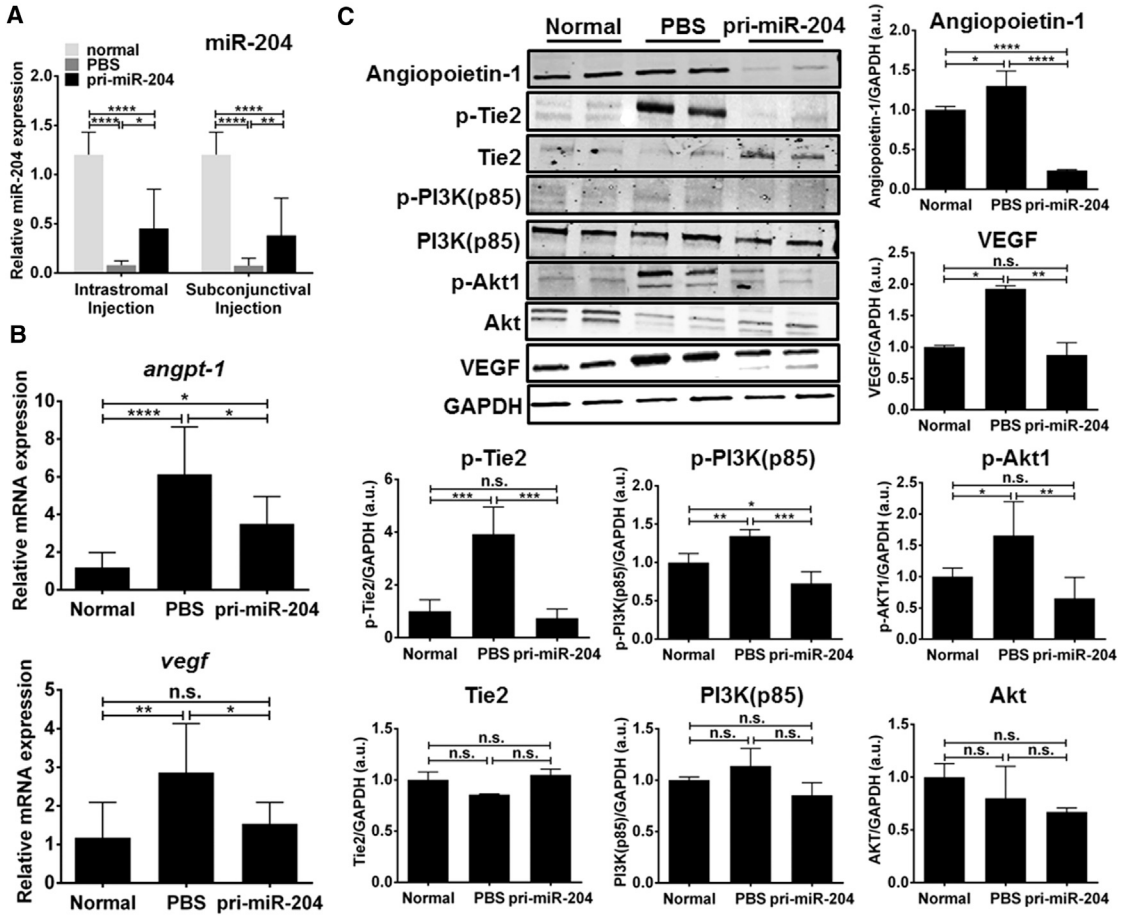

Figure 6. The Anti-angiogenic Effect of Overexpressing miR-204 Is Due in Part to Targeting the Angpt1/Tie2/PI3K/Akt Pathway

(A) Real-time qPCR analysis of miR-204 expression in mouse corneas by intrastromal or subconjunctival injection. (B) Real-time qPCR analysis of *angpt1* and *vegf* mRNA expression. (C) Western blot analysis of ANGPT1 and VEGF expression, and the phosphorylation states of key factors in the Tie2/PI3K/Akt pathway. n = 6/group. Error bars are ± SD. The notably large SD values observed are due to the variability inherent to *in vivo* experiments and the relatively small quantity of protein and mRNA obtained from mouse corneas. n.s., no significant difference. *p < 0.05; **p < 0.01; ***p < 0.001; ****p < 0.0001.

(Phoenix Research Labs, Pleasanton, CA, USA). The area of corneal NV was calculated by using the following formula modified from Liu et al.[27] Area (mm^2) = CN/12 × 3.1416 × [R^2 − (R − VL)^2], where CN is the clock-hours of NV (1 clock-hour equals 30 degrees of arc); R is the radius of the cornea; and VL is the maximal vessel length, extending from the limbal vasculature. Measurements of corneas in live animals were performed five times each under a Micron III microscope, and the area of corneal NV was calculated accordingly.

NanoString nCounter miRNA Assay for miRNA Profiling

A total of 100 ng of RNA was extracted from whole mouse corneas. Four corneas were pooled into one sample. Two samples for each time point (eight corneas each) were profiled for miRNA expression using the nCounter miRNA Expression Assay Kit (NanoString Technologies, Seattle, WA, USA). The assay was performed according to the manufacturer's instructions, querying 578 mouse miRNA targets, 33 mouse-associated viral miRNA targets, and 6 negative control targets. The mean expression values of each miRNA were calculated by normalizing across our cohort to filter for expressed miRNAs. The six internal negative control probes served as the background threshold cutoff point (set to 1.0).

RNA-Seq

Mouse corneas representing three treatment groups were treated as above: non-treated (day 0), post-operative (day 5), and regression post-operative (day 15). Whole corneal tissues were sent on dry ice to Otogenetics (Atlanta, GA, USA). Total RNA was extracted from tissues and processed for RNA-seq library preparation and high-throughput sequencing on a HiSeq2500 platform following Otogenetics' standard pipelines. Four corneas were pooled to represent a single sample library, and two libraries represent each treatment condition. Each biological condition therefore reflects eight individual mouse corneas. This strategy was employed to compensate for the

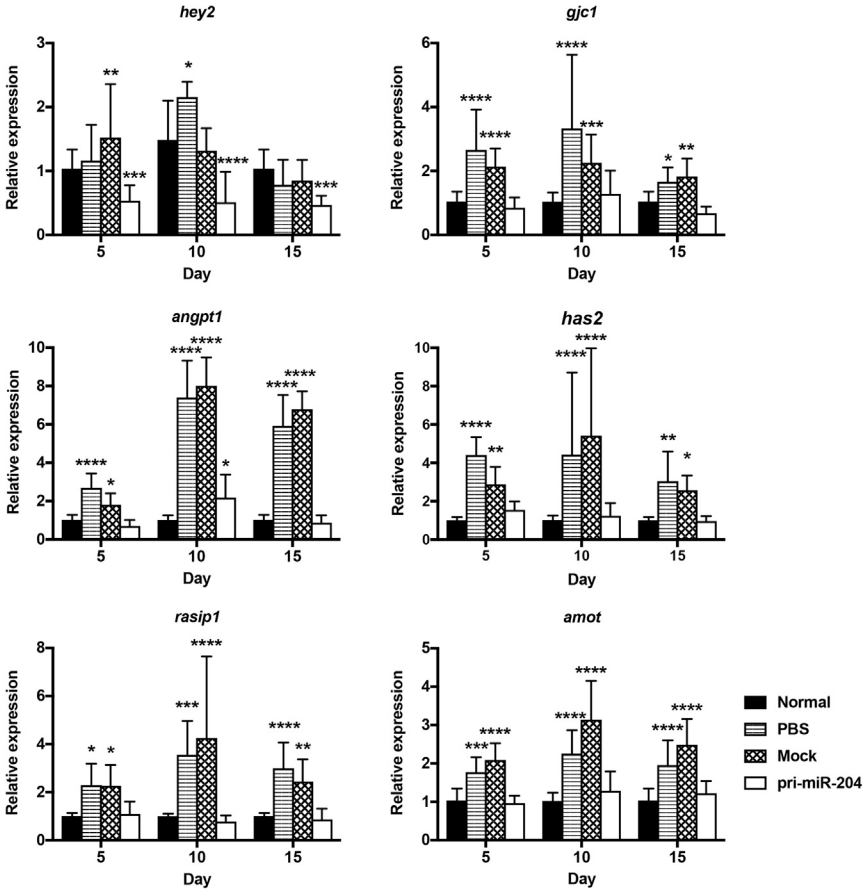

Figure 7. Predicted Corneal NV miR-204 Gene Targets Are Normalized following Treatment with rAAVrh.10 Pri-miR-204

Alkali-burn-treated mouse eyes were subconjunctivally injected with PBS, mock, or pri-miR-204. After 5, 10, or 15 days following treatment, corneas were obtained for qPCR analysis. At least five eyes per group were analyzed (3 days with four treatment conditions, 12 groups total). qPCR analysis of target transcripts in triplicate were conducted. The mean fold-change of message levels as compared with the normal groups ± SD is displayed. The notably large SD values observed are due to the variability inherent to *in vivo* experiments and the relatively small quantity of protein and mRNA obtained from mouse corneas. *p < 0.05; **p < 0.01; ***p < 0.001; ****p < 0.0001, two-way ANOVA.

low abundance of total RNA in an individual mouse cornea and to limit the number of animals used for each condition. Primary bioinformatics analysis (Tophat/Cufflinks workflows,[28] differential expression, and ontology enrichment analysis) was performed by ContigExpress (New York, NY, USA). Predicted miRNA target genes were selected from differentially expressed genes and analyzed with the CummeRbund (v2.12.1) software package.[28]

Bioinformatics Analysis

Hierarchical Cluster Analysis

Hierarchical clustering was performed with average linkage using Cluster 3.0 (Eisen Lab, University of California at Berkeley, CA, USA). The clustered heatmap was visualized using the interactive graphical software, TreeView (Eisen Lab). A limma algorithm was applied to filter the differentially expressed miRNAs from different experimental groups.[29] After performing significance ($p < 0.05$) and false discovery rate analysis (FDR < 0.05), we selected differentially expressed miRNAs with a ±2-fold change cutoff. Selected miRNAs were ranked by fold-change.

miRNA Target Gene Prediction and GO/Pathway Analysis

Differentially expressed miRNAs identified by nCounter Analysis were subjected to target gene prediction analysis using TargetScan and miRTarBase definitions.[30,31] GO network maps and term enrichment analyses were performed using Cytoscape_v3.3.0 plug-in tools and ClueGO v2.2.3[32] with terms defined by GO_BiologicalProcess-GOA_07.12.2015 and KEGG pathways. Significance was defined by a Kappa score threshold of 0.4, with p value cutoffs of 0.05 for pathway reporting. For reasons of practicality, only genes and miRNAs enriching for terms related to vasculogenesis, JAK-STAT signaling, Ephrin signaling, eye development, epithelial cell homeostasis, bone morphogenetic protein (BMP) signaling, wound healing, and cell growth were reported.

Data Reporting

The nCounter and RNA-seq data discussed in this publication have been deposited in NCBI's GEO and are accessible through GEO: GSE89538 (https://www.ncbi.nlm.nih.gov/geo/query/acc.cgi?acc=GSE89538).

rAAV Vector Production

pri-miR-184 and pri-miR-204 were amplified using the PrimeSTAR Max DNA Polymerase kit (Takara, Japan) with the following primers: pri-miR-184, sense 5′-ccggaattctgtgcagaaacataagtgactctccaggtg-3′, antisense 5′-atcggcggccgcgcagagagcacattttgaataagcaaagtg-3′; pri-miR-204, sense 5′-ccggaattctttacccacaggacagggtgatggagagga-3′, antisense 5′-atcggcggccgcgtcacatggtttggacccagaactattagt-3′.

PCR products were sub-cloned into the self-complementary (sc) pAAV-CB-PI-GaussiaLuc plasmid by conventional means using NotI and EcoRI restriction sites. The sc-pAAV-CB-PI-EGFP plasmid and sc-pAAV-CB-PI-pri-miR184/204-GaussiaLuc plasmids were packaged with rAAVrh.10 capsids by triple-plasmid transfection of HEK293 cells.[22,33] Viruses were purified with CsCl gradient ultracentrifugation and titered by both qPCR and silver staining of SDS-PAGE gels.[33]

Table 1. Primer Sequences in This Study

Gene	Forward Primer Sequence (5′-3′)	Reverse Primer Sequence (5′-3′)
fzd4	TGCCAGAACCTCGGCTACA	ATGAGCGGCGTGAAAGTTGT
vegf-a	GCCAGCACATAGAGAGAATGAGC	CAAGGCTCACAGTGATTTTCTGG
angpt1	CACATAGGGTGCAGCAACCA	CGTCGTGTTCTGGAAGAATGA
hey2	CACTGGGACAAACAATAAAC	TCTGTATGACTACCTTCAGG
gjc1	TGAGGTGGGCTTTCTAATAG	TATGAGGGCAAGGAAGTCTG
angpt1*	GGTGCTCTGCCAGTATTAGA	TGACATAACCACTTGCTGCT
has2	GACGGTGGGATGATGTCTT	ACAAACACTGTCAGGCAGAT
Rasip1	GACCTCGTGTCCCAGACTT	GACCTCGTTCCATCAGTGAG
Amot	CGTCCACTAGATTGCCTCCT	CGAAAGAAGATGCTGCTGAT
β-actin	CCTCTATGCCAACACAGT	AGCCACCAATCCACACAG

amot, Angiomotin; angpt1, angiopoitein-1; angpt1*, alternative primer set for angpt1 used in Figure 7; β-actin, Beta-actin; fzd4, frizzled receptor-4; gjc1, Gap junction gamma-1 protein; has2, Hyaluronan synthase 2; hey2, Hes-Related Family BHLH Transcription Factor With YRPW Motif 2; rasip1, Ras-interacting protein 1; vegf-a, vascular endothelial growth factor-a.

rAAV Transduction by Intrastromal or Subconjunctival Injection

Intrastromal injections were performed following previously published methods.[22] In brief, a 1.0-mm-long incision using the tip of a 26-gauge needle was first created through the corneal epithelium, equidistant between the cornea-scleral junction and the corneal center. Then, 3.6×10^{10} genomic copies (GCs) of vector in 4 μL of PBS were injected through the incision into the corneal stroma using a 33-gauge needle and a 5-μL Hamilton syringe (Hamilton, Reno, NV, USA). Subconjunctival injections were performed using a 5-μL Hamilton syringe to deliver 3.6×10^{10} GCs of vector in 4 μL of PBS. Antibiotic ointment was applied after injections.

Real-Time qPCR for miRNA and mRNA Expression Analyses

RNA extraction and real-time qPCR for miRNA (TaqMan miRNA assay; miR-184, miR-204; Life Technologies, Carlsbad, CA, USA) and mRNAs were performed as described previously.[34] Primer sequences for *fzd4*, *vegf-a*, and *angpt1* are reported in Table 1. Primer sets for hey2, gjc1, angpt1, has2, rasip1, amot, and β-actin used in Figure 7 were designed and synthesized by BioTNT (http://www.biotnt.us). *U6* and *β-actin* were used as normalization transcripts for miRNAs and mRNAs, respectively.

Droplet Digital PCR for rAAV Genome Copy Number and RNA Expression Analyses

Mouse cornea genomic DNA was isolated using the QIAamp DNA kit (QIAGEN, Hilden, Germany) following manufacturer's instructions and then digested with >10 U/μg SalI (New England Biolabs, Ipswich, MA, USA) at 37°C for 1 hr. There are two SalI sites in the rAAV genome, and SalI digestion ensures single copy emulsion for droplet digital PCR (ddPCR) quantification. Multiplexed ddPCR was performed on a QX200 ddPCR system (Bio-Rad Laboratories, Hercules, CA, USA) using TaqMan reagents targeting EGFP (catalog no. 4400293; Life Technologies) and the reference gene, transferrin receptor (Tfrc) (catalog no. 4458367; Invitrogen, Waltham, MA, USA). rAAV genome copy numbers per diploid genome were calculated as *EGFP* transgene copy numbers per two *Tfrc* gene copies.

Total RNA was extracted using the RNeasy 96 QIAcube HT kit with on-column DNase I digestion (QIAGEN, Valencia, CA, USA), reverse-transcribed into cDNA, and subjected to multiplexed ddPCR using TaqMan reagents targeting *EGFP* and Glyceraldehyde-3-Phosphate Dehydrogenase (*gapdh*) (catalog no. 4352339E; Life Technologies). The quantity of *EGFP* was normalized to *gapdh* levels.

Western Blot

Total protein from corneas was extracted on ice with RIPA lysis buffer in the presence of freshly added protease and phosphatase inhibitors (Thermo Fisher Scientific, Waltham, MA, USA). A total of 10 μg/lane protein extract was loaded onto a 4%–20% gradient SDS-polyacrylamide gel and transferred to nitrocellulose membranes (Bio-Rad Laboratories). Nonspecific binding was blocked with 5% nonfat milk or 5% BSA in Tris-buffered saline with Tween20 (TBST) as recommended for each antibody. The membrane was incubated with rabbit anti-VEGF (ab46154; Abcam, Cambridge, MA, USA), anti-Angpt1 (ab95230; Abcam), anti-Tie2 (catalog [Cat.] no. 7403; Cell Signaling, Danvers, MA, USA), anti-phospho-Tie2 (AF2720-SP; R&D Systems, Minneapolis, MN, USA), anti-PI3K (p85) (Cat. no. 4292; Cell Signaling), anti-phospho-PI3K (p85) (Cat. no. 4228; Cell Signaling), anti-Akt (ab8805; Abcam), anti-phospho-Akt1 (ab81283; Abcam), anti-Fzd4 (ab83042; Abcam), anti-LRP6 (Cat. no. 3395S; Cell Signaling), anti-phospho-LRP6 (Cat. no. 2568S; Cell Signaling), anti-N-p-β-catenin (Cat. no. 4270; Cell Signaling), or anti-β-catenin (Cat. no. 8480S; Cell Signaling) antibodies overnight at 4°C. IRDye 800CW goat anti-rabbit IgG (Cat. no. 926-32211; LI-COR, Lincoln, NE, USA) was used as the secondary antibody, and mouse anti-GAPDH antibody (ab8245; Abcam) was used as an internal standard.

Histological and Immunofluorescence-Histochemical Analyses

For rAAV transduction efficiency analysis, mouse eyes were enucleated and fixed in 4% paraformaldehyde. Corneas with limbi were then harvested for corneal flat-mounts and blocked in 5% goat serum in PBS.

For detecting EGFP expression in normal mouse corneas, flat-mounts were stained with rabbit anti-mouse GFP primary antibody (1:1,000; Life Technologies), followed by goat anti-rabbit IgG-Alexa Fluor 488 secondary antibody (1:1,500; Life Technologies). For corneas treated by alkali burn, flat-mounts were stained with rat anti-mouse CD31 (1:500; Abcam) and rabbit anti-mouse keratocan (1:50; Santa Cruz Biotechnology, Dallas, TX, USA) primary antibodies, followed by goat anti-rat IgG-Alexa Fluor 568 and goat anti-rabbit IgG-Alexa Fluor 694 secondary antibodies (1:1,500; Life Technologies). Corneal whole mounts were set with VECTASHIELD anti-fade mounting medium with DAPI (Vector Laboratories, Burlingame, CA, USA) for observation and imaging analysis. For corneal NV detection after alkali-burn treatment, flat-mounts were stained with the rat anti-mouse CD31 primary antibody (1:5,00; Abcam), followed by goat anti-rat IgG-Alexa Fluor 568 secondary antibody (1:1,500).

To evaluate the safety of pri-miRNA vectors, we fixed mouse eyes from each group in 10% formalin, embedded in paraffin, sectioned at a thickness of 4 μm, and stained with H&E for histological analysis. Images were obtained using a Leica DMC2900 microscope (Leica Microsystems, Buffalo Grove, IL, USA).

Statistical Analysis

Results are expressed as mean ± SD. Analysis was performed with one-way or two-way ANOVA for multiple variables, and Bonferroni's post hoc multiple-comparison test was used for inter-group differences using GraphPad Prism 6.0 (GraphPad Software, La Jolla, CA, USA). $p < 0.05$ was considered significant in all cases. p values for Figures 6 and 7 are included in the Supplemental Information as Tables S3 and S4, respectively.

SUPPLEMENTAL INFORMATION

Supplemental Information includes six figures and four tables and can be found with this article online at https://doi.org/10.1016/j.omtn.2017.12.019.

AUTHOR CONTRIBUTIONS

Y.L., P.D.Z., X.X., and G.G. designed the experiments. Y.L., P.W.L.T., J.A., D.J.G., Q.S., X.Y., and Q.Z. performed the experiments. Y.L. and D.J.G. performed the NanoString nCounter data analysis. P.W.L.T. performed the RNA-seq data analysis. D.J.G. helped with manuscript editing. Y.L. and P.W.L.T. prepared the figures. Y.L., P.W.L.T., and G.G. wrote the manuscript.

CONFLICTS OF INTEREST

G.G. and P.D.Z. are co-founders of Voyager Therapeutics and hold equity in the company. G.G. is an inventor on patents with potential royalties licensed to Voyager Therapeutics and other biopharmaceutical companies. Q.Z. is a salaried employee of the Kanghong Pharmaceutical Group Co., Ltd.

ACKNOWLEDGMENTS

This work was supported by a research grant from The National Key Research and Development Program of China (2016YFC0904800), The National Natural Science Foundation of China (81570851), and an internal grant from Shanghai Jiaotong University School of Medicine (20161426) to X.X. and Y.L.; a corporate-sponsored research grant from Chengdu Kanghong Pharmaceutical Group Co., Ltd. to G.G., X.X., and Q.Z.; an internal grant from the University of Massachusetts Medical School; and research grants from the NIH (R01NS076991-01, 1P01AI100263-01, R01 HL097088, and P01HL131471-01) to G.G.

REFERENCES

1. Whitcher, J.P., Srinivasan, M., and Upadhyay, M.P. (2001). Corneal blindness: a global perspective. Bull. World Health Organ. *79*, 214–221.
2. Chang, J.H., Garg, N.K., Lunde, E., Han, K.Y., Jain, S., and Azar, D.T. (2012). Corneal neovascularization: an anti-VEGF therapy review. Surv. Ophthalmol. *57*, 415–429.
3. Oh, J.Y., Kim, M.K., Shin, M.S., Lee, H.J., Ko, J.H., Wee, W.R., and Lee, J.H. (2008). The anti-inflammatory and anti-angiogenic role of mesenchymal stem cells in corneal wound healing following chemical injury. Stem Cells *26*, 1047–1055.
4. Ellenberg, D., Azar, D.T., Hallak, J.A., Tobaigy, F., Han, K.Y., Jain, S., Zhou, Z., and Chang, J.H. (2010). Novel aspects of corneal angiogenic and lymphangiogenic privilege. Prog. Retin. Eye Res. *29*, 208–248.
5. Akar, E.E., Oner, V., Küçükerdönmez, C., and Aydın Akova, Y. (2013). Comparison of subconjunctivally injected bevacizumab, ranibizumab, and pegaptanib for inhibition of corneal neovascularization in a rat model. Int. J. Ophthalmol. *6*, 136–140.
6. Papathanassiou, M., Theodossiadis, P.G., Liarakos, V.S., Rouvas, A., Giamarellos-Bourboulis, E.J., and Vergados, I.A. (2008). Inhibition of corneal neovascularization by subconjunctival bevacizumab in an animal model. Am. J. Ophthalmol. *145*, 424–431.
7. Voiculescu, O.B., Voinea, L.M., and Alexandrescu, C. (2015). Corneal neovascularization and biological therapy. J. Med. Life *8*, 444–448.
8. Anand, S., and Cheresh, D.A. (2011). Emerging role of micro-RNAs in the regulation of angiogenesis. Genes Cancer *2*, 1134–1138.
9. Hassel, D., Cheng, P., White, M.P., Ivey, K.N., Kroll, J., Augustin, H.G., Katus, H.A., Stainier, D.Y., and Srivastava, D. (2012). MicroRNA-10 regulates the angiogenic behavior of zebrafish and human endothelial cells by promoting vascular endothelial growth factor signaling. Circ. Res. *111*, 1421–1433.
10. Ben-Hamo, R., and Efroni, S. (2015). MicroRNA regulation of molecular pathways as a generic mechanism and as a core disease phenotype. Oncotarget *6*, 1594–1604.
11. Liu, C.H., Sun, Y., Li, J., Gong, Y., Tian, K.T., Evans, L.P., Morss, P.C., Fredrick, T.W., Saba, N.J., and Chen, J. (2015). Endothelial microRNA-150 is an intrinsic suppressor of pathologic ocular neovascularization. Proc. Natl. Acad. Sci. USA *112*, 12163–12168.
12. Zong, R., Zhou, T., Lin, Z., Bao, X., Xiu, Y., Chen, Y., Chen, L., Ma, J.X., Liu, Z., and Zhou, Y. (2016). Down-regulation of microRNA-184 is associated with corneal neovascularization. Invest. Ophthalmol. Vis. Sci. *57*, 1398–1407.
13. Gupta, D., and Illingworth, C. (2011). Treatments for corneal neovascularization: a review. Cornea *30*, 927–938.
14. Mohan, R.R., Rodier, J.T., and Sharma, A. (2013). Corneal gene therapy: basic science and translational perspective. Ocul. Surf. *11*, 150–164.
15. Mohan, R.R., Tovey, J.C., Sharma, A., and Tandon, A. (2012). Gene therapy in the cornea: 2005—present. Prog. Retin. Eye Res. *31*, 43–64.
16. Wang, D., and Gao, G. (2014). State-of-the-art human gene therapy: part II. Gene therapy strategies and clinical applications. Discov. Med. *18*, 151–161.
17. Wang, D., and Gao, G. (2014). State-of-the-art human gene therapy: part I. Gene delivery technologies. Discov. Med. *18*, 67–77.
18. Gerlach, D., Kriventseva, E.V., Rahman, N., Vejnar, C.E., and Zdobnov, E.M. (2009). miROrtho: computational survey of microRNA genes. Nucleic Acids Res. *37*, D111–D117.
19. An, J., Chen, X., Chen, W., Liang, R., Reinach, P.S., Yan, D., and Tu, L. (2015). MicroRNA expression profile and the role of miR-204 in corneal wound healing. Invest. Ophthalmol. Vis. Sci. *56*, 3673–3683.

20. Kather, J.N., Friedrich, J., Woik, N., Sticht, C., Gretz, N., Hammes, H.P., and Kroll, J. (2014). Angiopoietin-1 is regulated by miR-204 and contributes to corneal neovascularization in KLEIP-deficient mice. Invest. Ophthalmol. Vis. Sci. *55*, 4295–4303.

21. Hippert, C., Ibanes, S., Serratrice, N., Court, F., Malecaze, F., Kremer, E.J., and Kalatzis, V. (2012). Corneal transduction by intra-stromal injection of AAV vectors in vivo in the mouse and ex vivo in human explants. PLoS ONE *7*, e35318.

22. Lu, Y., Ai, J., Gessler, D., Su, Q., Tran, K., Zheng, Q., Xu, X., and Gao, G. (2016). Efficient transduction of corneal stroma by adeno-associated viral serotype vectors for implications in gene therapy of corneal diseases. Hum. Gene Ther. *27*, 598–608.

23. Fasciani, R., Mosca, L., Giannico, M.I., Ambrogio, S.A., and Balestrazzi, E. (2015). Subconjunctival and/or intrastromal bevacizumab injections as preconditioning therapy to promote corneal graft survival. Int. Ophthalmol. *35*, 221–227.

24. Fagiani, E., and Christofori, G. (2013). Angiopoietins in angiogenesis. Cancer Lett. *328*, 18–26.

25. Wang, X., Li, J., Wu, D., Bu, X., and Qiao, Y. (2016). Hypoxia promotes apoptosis of neuronal cells through hypoxia-inducible factor-1α-microRNA-204-B-cell lymphoma-2 pathway. Exp. Biol. Med. (Maywood) *241*, 177–183.

26. Ferrari, G., Bignami, F., Giacomini, C., Franchini, S., and Rama, P. (2013). Safety and efficacy of topical infliximab in a mouse model of ocular surface scarring. Invest. Ophthalmol. Vis. Sci. *54*, 1680–1688.

27. Liu, X., Lin, Z., Zhou, T., Zong, R., He, H., Liu, Z., Ma, J.X., Liu, Z., and Zhou, Y. (2011). Anti-angiogenic and anti-inflammatory effects of SERPINA3K on corneal injury. PLoS ONE *6*, e16712.

28. Trapnell, C., Roberts, A., Goff, L., Pertea, G., Kim, D., Kelley, D.R., Pimentel, H., Salzberg, S.L., Rinn, J.L., and Pachter, L. (2012). Differential gene and transcript expression analysis of RNA-seq experiments with TopHat and Cufflinks. Nat. Protoc. *7*, 562–578.

29. Wettenhall, J.M., and Smyth, G.K. (2004). limmaGUI: a graphical user interface for linear modeling of microarray data. Bioinformatics *20*, 3705–3706.

30. Vlachos, I.S., Paraskevopoulou, M.D., Karagkouni, D., Georgakilas, G., Vergoulis, T., Kanellos, I., Anastasopoulos, I.L., Maniou, S., Karathanou, K., Kalfakakou, D., et al. (2015). DIANA-TarBase v7.0: indexing more than half a million experimentally supported miRNA:mRNA interactions. Nucleic Acids Res. *43*, D153–D159.

31. Peterson, S.M., Thompson, J.A., Ufkin, M.L., Sathyanarayana, P., Liaw, L., and Congdon, C.B. (2014). Common features of microRNA target prediction tools. Front. Genet. *5*, 23.

32. Bindea, G., Mlecnik, B., Hackl, H., Charoentong, P., Tosolini, M., Kirilovsky, A., Fridman, W.H., Pagès, F., Trajanoski, Z., and Galon, J. (2009). ClueGO: a Cytoscape plug-in to decipher functionally grouped gene ontology and pathway annotation networks. Bioinformatics *25*, 1091–1093.

33. Gao, G.P., and Sena-Esteves, M. (2012). Introducing genes into mammalian cells: viral vectors. In Molecular Cloning, Vol. 2: A Laboratory Manual, M.R. Green and J. Sambrook, eds. (Cold Spring Harbor Laboratory Press), pp. 1209–1313.

34. Xie, J., Ameres, S.L., Friedline, R., Hung, J.H., Zhang, Y., Xie, Q., Zhong, L., Su, Q., He, R., Li, M., et al. (2012). Long-term, efficient inhibition of microRNA function in mice using rAAV vectors. Nat. Methods *9*, 403–409.